Current Distribution Optimization by Using Genetic-Algorithm Based On-Off Method: Application to Pellet Injection System

Current Distribution Optimization by Using Genetic-Algorithm Based On-Off Method: Application to Pellet Injection System

Takazumi Yamaguchi[1,*], Hiroaki Ohtani[1,2], Teruou Takayama[3], Atsushi Kamitani[3]

[1]School of Physical Sciences, The Graduate University for Advanced Studies
[2]National Institute for Fusion Science
[3]Graduate School of Science and Engineering, Yamagata University

*yamaguchi.takazumi@nifs.ac.jp

Abstract. The current distribution in the electromagnet is optimized by using the genetic-algorithm based on-off method so as to maximize the acceleration performance of the Superconducting Linear Acceleration (SLA) system. In the SLA system, a pellet container is accelerated by the interaction between a shielding current density and an applied magnetic field. By using the equivalent-circuit model, the distribution of the shielding current density is approximated as a set of the multiple current loops. In contrast, the current distribution in the electromagnet is represented by means of the on-off method. As the method for optimizing the current distribution in the electromagnet, two types of genetic algorithms are adopted. The results of computations show that the pellet velocity for the optimized current distribution is 1.3 times as fast as that for the homogeneous current distribution.

Keywords: current distribution optimization, equivalent-circuit model, high-temperature superconductor, NSGA-II, on-off method, weighted GA

1. Introduction

Nuclear fusion energy has attracted great attention as an alternative energy source. In order to realize the nuclear fusion, it is essential to continuously maintain ultra-high-temperature plasma. To this end, a fuel pellet is directly injected into the core plasma. According to the study of the pellet-plasma interaction [1, 2], the pellet can reach to the core plasma if and only if its velocity exceeds 5 km/s. Otherwise, the pellet melts near the plasma edge. Currently, a pneumatic pipe-gun type system is used as the pellet injection system for the Large Helical Device (LHD). However, the pneumatic system accelerates a pellet only up to 3 km/s [3]. In this sense, the pellet injection by the pneumatic system is not sufficiently efficient for the pellet supply to the LHD.
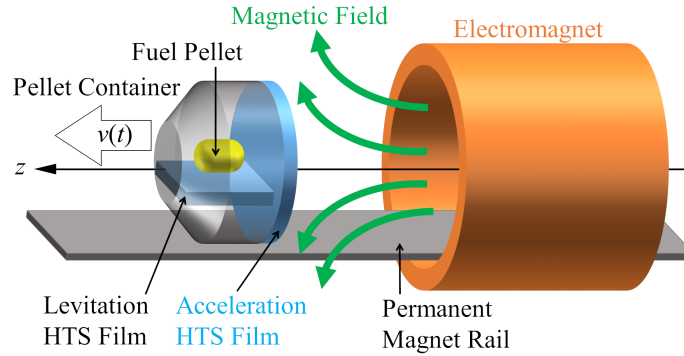
Figure 1: A schematic view of the SLA system.

For the purpose of overcoming the above problem, the Superconducting Linear Acceleration (SLA) system has been recently proposed [4]. The SLA system is composed of an electromagnet and a pellet container to which a High-Temperature Superconducting (HTS) film is attached. The SLA system accelerates the container by using an electromagnetic force and injects the pellet into the core plasma. According to the rough estimation [4], the SLA system might accelerate the container up to 5 km/s. However, the acceleration performance of the SLA system is not clarified because the SLA experiment has not been performed yet.

In the previous study, the authors proposed the Equivalent-Circuit Model (ECM) to analyze a shielding current density in an axisymmetric HTS film [5, 6]. By using the ECM, they numerically investigated the acceleration performance of the SLA system for the multiple electromagnets. As a result, it was found that a considerable number of the electromagnets must be placed over 40 km to increase the pellet velocity up to 5 km/s [6]. Accordingly, it is essential to improve the acceleration performance of each electromagnet.

The purpose of the present study is to develop the ECM code for analyzing a shielding current density for an arbitrarily current distribution in the electromagnet. Moreover, by combining the ECM code with the Genetic Algorithm (GA), we optimize the current distribution in the electromagnet so as to maximize the acceleration performance of a single electromagnet.

2.   Numerical Method

In the present study, the acceleration performance of the SLA system is analyzed by using the ECM. To this end, the current distribution in the electromagnet is represented by means of the on-off method. In this section, after the ECM and the on-off method are introduced, the governing equations and their solution are explained.
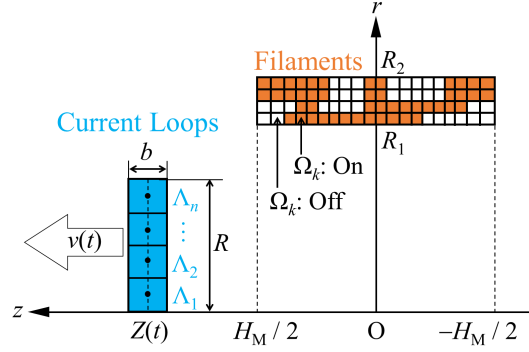
Figure 2: An equivalent-circuit model.

2.1. Equivalent-Circuit Model

A schematic view of the SLA system is shown in Fig. 1. A fuel pellet is carried by the pellet container to which both an acceleration HTS film and a levitation HTS film are attached. The container is levitated by the repulsive force between the levitation HTS film and the permanent-magnet rail. In addition, the acceleration HTS film is exposed to the magnetic flux density generated by an electromagnet. As a result, the Lorentz force acts on the acceleration HTS film to speed up the container.

Throughout the present study, the shape of the acceleration HTS film is assumed to be a disk of radius R and thickness b. We further assume that the axisymmetric magnetic flux density is generated by the cylindrical electromagnet of inner radius R_1, outer radius R_2, and length H_M (see Fig. 2). For simplicity, neither the permanent-magnet rail nor the levitation HTS film are taken into consideration in the ECM.

Under the above assumptions, the distribution of the shielding current density in the acceleration HTS film can be approximated as a set of n current loops, $\Lambda_1, \Lambda_2, \cdots, \Lambda_n$ (see Fig. 2). Here, Λ_i is the ith current loop with a rectangular cross section of width $\Delta r \ (\equiv R/n)$ and thickness b. In addition, r- and z-coordinates of the center in the cross section of Λ_i are denoted by r_i and $Z(t)$, respectively. Thus, $Z(t)$ is the position of the acceleration HTS film. In the following, the electric current and the voltage in Λ_i are denoted by I_i and V_i, respectively.

2.2. On-Off Method

In order to implement the on-off method to the ECM, the electromagnet is radially and longitudinally divided into K_r and K_z parts, respectively. Thus, the electromagnet is approximated as a set of K filaments, $\Omega_1, \Omega_2, \cdots, \Omega_K$ (see Fig. 2), where $K \equiv K_r K_z$. If an electric current flows in Ω_k, Ω_k is called on-state. Otherwise, Ω_k is called off-state. In other words, the current distribution is represented in terms of a K-dimensional state vector:

$$\boldsymbol{x} \equiv (x_1, x_2, \cdots, x_K)^{\mathrm{T}}, \tag{1}$$

3

where x_k is defined by

$$x_k \equiv \begin{cases} 1 & (\Omega_k : \text{on-state}) \\ 0 & (\Omega_k : \text{off-state}) \end{cases}. \tag{2}$$

By using the state vector $\boldsymbol{x}$, electric currents in all the filaments are represented by

$$\boldsymbol{I}_{\text{F}}(t, Z) \equiv \frac{I_{\text{total}}(t, Z)}{K} \boldsymbol{x}, \tag{3}$$

where the kth component of $\boldsymbol{I}_{\text{F}}(t, Z)$ denotes an electric current in Ω_k. In addition, $I_{\text{total}}(t, Z)$ is a total current in the electromagnet for the case where all the filaments are on-state. Throughout the present study, $I_{\text{total}}(t, Z)$ is assumed as

$$I_{\text{total}}(t, Z) = \begin{cases} \alpha t & (0 \leq Z \leq z_{\text{limit}}) \\ 0 & (\text{otherwise}) \end{cases}, \tag{4}$$

where α is an increasing rate of $I_{\text{total}}(t, Z)$. Note that, only when the inequality $0 \leq Z \leq z_{\text{limit}}$ is fulfilled, an electric current flows in the on-state filaments. In other words, an acceleration range is represented by $0 \leq z \leq z_{\text{limit}}$.

2.3. Governing Equations

By using the ECM and the on-off method, Faraday's law becomes equivalent to the following circuit equation:

$$L\frac{d\boldsymbol{I}}{dt} = -\left[\boldsymbol{M}(Z)\frac{dI_{\text{total}}}{dt} + \frac{d\boldsymbol{M}}{dZ} v I_{\text{total}} + \boldsymbol{V} \right], \tag{5}$$

where $\boldsymbol{I}$, $\boldsymbol{V}$, and $\boldsymbol{M}$ are defined by $\boldsymbol{I} \equiv (I_1, I_2, \cdots, I_n)^{\text{T}}$, $\boldsymbol{V} \equiv (V_1, V_2, \cdots, V_n)^{\text{T}}$, and $\boldsymbol{M}(Z) \equiv M(Z)\boldsymbol{x}/K$. Moreover, $L \in \mathbb{R}^{n \times n}$ is an inductance matrix whose (i, j)th entry is the inductance by Λ_j on Λ_i. Furthermore, $M(Z) \in \mathbb{R}^{n \times K}$ is a mutual-inductance matrix whose (i, k)th entry is the mutual inductance by Ω_k on Λ_i. In addition, v ($\equiv dZ/dt$) is the velocity of the HTS film. In order to determine the induced voltage V_i in Λ_i, we adopt the power law [5, 7, 8]:

$$V_i = V_{\text{C}i}\left(\frac{|I_i|}{I_\text{C}}\right)^N \text{sgn}(I_i), \tag{6}$$

where $V_{\text{C}i} \equiv 2\pi(r_i + \Delta r/2)E_\text{C}$ and $I_\text{C} \equiv b\Delta r j_\text{C}$. Here, E_C and j_C denote a critical electric field and a critical current density, respectively, and N is a positive constant. The power law (6) shows the superconducting characteristics in Λ_i.

The dynamic motion of the container is governed by Newton's equation of motion:

$$m\frac{d^2Z}{dt^2} = -2\pi \sum_{i=1}^{n} r_i B_r(Z, r_i, t)I_i, \tag{7}$$

where m is a total mass of the container and the HTS films. Also, $B_r(z, r, t)$ is r-component of the magnetic flux density generated by the electromagnet. Incidentally, the effect of air resistance is neglected in (7). This is mainly because the SLA experiment is performed under extremely low pressure.

Rewriting (5) and (7), we obtain the following first-order ordinary differential equations:

$$\frac{d}{dt}\begin{pmatrix} \boldsymbol{I} \\ v \\ Z \end{pmatrix} = \begin{pmatrix} -L^{-1}\left[\boldsymbol{M}(Z)\dfrac{dI_{\text{total}}}{dt} + \dfrac{d\boldsymbol{M}}{dZ}\, v\, I_{\text{total}} + \boldsymbol{V} \right] \\ -\dfrac{2\pi}{m}\displaystyle\sum_{i=1}^{n} r_i B_r(Z, r_i, t)I_i \\ v \end{pmatrix}. \tag{8}$$

The initial conditions to (8) are assumed as follows:

$$\boldsymbol{I} = \boldsymbol{0},\ v = 0\text{ m/s},\ \text{and}\ Z = z_0\ \text{at}\ t = 0. \tag{9}$$

Here, z_0 denotes an initial position of the HTS film. By solving an initial-value problem of (8), both the time evolution of the shielding current density and the dynamic motion of the container can be determined simultaneously. Throughout the present study, the initial-value problem of (8) is solved by means of the 5th-order Runge-Kutta method with the adaptive step-size control algorithm [9, 10].

3. Optimization Method

In optimizing the current distribution in the electromagnet, the state vector $\boldsymbol{x}$ is determined so as to maximize the acceleration performance of the SLA system. As an optimization method, the weighted Genetic Algorithm (GA) and the Non-dominated Sorting Genetic Algorithm II (NSGA-II) [11] are adopted. In this section, we explain the objective functions and two types of GAs.

3.1. Objective Functions

In order to evaluate the acceleration performance quantitatively, we introduce the speedup ratio f_v and the on-ratio f_{on}. The speedup ratio $f_v(\boldsymbol{x})$ is defined by

$$f_v(\boldsymbol{x}) \equiv \frac{v_f(\boldsymbol{x})}{v_{\text{ref}}}, \tag{10}$$

where $v_f(\boldsymbol{x})$ and v_{ref} are the final velocity for the state vector $\boldsymbol{x}$ and that for the homogeneous current distribution, respectively. Here, the final velocity is the value of $v(t)$ at the time when $Z(t) = z_{\text{limit}}$ is satisfied. Both $v_f(\boldsymbol{x})$ and v_{ref} are determined by using the ECM. On the other hand, the on-ratio $f_{\text{on}}(\boldsymbol{x})$ is defined by

$$f_{\text{on}}(\boldsymbol{x}) \equiv \frac{K_{\text{on}}(\boldsymbol{x})}{K}, \tag{11}$$

where $K_{\text{on}}(\boldsymbol{x})$ is the number of on-state filaments.

In the following, the state vector $\boldsymbol{x}$ is determined so as to maximize $f_v(\boldsymbol{x})$ and to minimize $f_{\text{on}}(\boldsymbol{x})$. In other words, the state vector $\boldsymbol{x}$ is obtained by means of the multiobjective optimization. In both the weighted GA and the NSGA-II, the generation process is repeated until the number s of generations reaches up to s_{max}.

3.2. Weighted GA

In the weighted GA, the multiobjective optimization is transformed into the single-objective optimization by introducing a weighting coefficient ω. By using $f_v(\boldsymbol{x})$ and $f_{on}(\boldsymbol{x})$, a combined objective function $f(\boldsymbol{x})$ is defined as follows:

$$f(\boldsymbol{x}) \equiv \omega f_v(\boldsymbol{x}) - (1 - \omega) f_{on}(\boldsymbol{x}), \tag{12}$$

where $0 \leq \omega \leq 1$. The state vector $\boldsymbol{x}$ is determined so as to maximize $f(\boldsymbol{x})$.

In the weighted GA, the parent state vectors are first chosen from state vectors by the tournament selection. Just after that, the offspring state vectors are produced by using the uniform crossover and, subsequently, part of them are mutated randomly. In the following, the numbers of parent state vectors and that of offspring state vectors are denoted by N_p and N_o, respectively.

3.3. NSGA-II

As the other optimization method, we adopt the NSGA-II [11]. Since the NSGA-II can be applied to both maximization and minimization of objective functions, it is also applicable to the present study. In the NSGA-II, parent state vectors are chosen by means of both the non-dominated sorting and the crowding distance sorting. In this subsection, these two sorting methods are briefly explained in relation to $f_v(\boldsymbol{x})$ and $f_{on}(\boldsymbol{x})$.

In the non-dominated sorting, if both $f_v(\boldsymbol{x}) > f_v(\boldsymbol{y})$ and $f_{on}(\boldsymbol{x}) < f_{on}(\boldsymbol{y})$ are satisfied by two state vectors, $\boldsymbol{x}$ and $\boldsymbol{y}$, we define that $\boldsymbol{y}$ is dominated by $\boldsymbol{x}$. Otherwise, we define that $\boldsymbol{y}$ is not dominated by $\boldsymbol{x}$. By using the above definition, a set T of state vectors is classified into the subsets, $F_1, F_2, \cdots, F_l$. First, F_1 is determined so that its elements may not be dominated by any state vector in T. Next, F_2 is determined so that its elements may not be dominated by any state vector in $T - F_1$. Similarly, F_3 is determined so that its elements may not be dominated by any state vector in $T - (F_1 + F_2)$. The above procedure is repeated until $T - (F_1 + F_2 + \cdots + F_l) = \phi$ is fulfilled. Here, ϕ denotes the empty set.

As is apparent from the above classification method, the optimum state vector always exists in F_1. Hence, in determining the optimum state vector at each generation, we need to check only the state vectors contained in F_1.

State vectors in each subset are further arranged by means of the crowding distance sorting. Specifically, they are sorted in the order of increasing crowding distance. For the state vector $\boldsymbol{x}_i \in F_e$, the crowding distance $d(\boldsymbol{x}_i)$ is determined by means of the following three steps:

1. The nearest state vectors, $\boldsymbol{x}_L, \boldsymbol{x}_R \in F_e$, which give the positive minimum values of $f_v(\boldsymbol{x}_i) - f_v(\boldsymbol{x}_L)$ and $f_v(\boldsymbol{x}_R) - f_v(\boldsymbol{x}_i)$, respectively, first are searched and, subsequently, $d_v(\boldsymbol{x}_i)$ is calculated by

$$d_v(\boldsymbol{x}_i) = \begin{cases} \dfrac{f_v(\boldsymbol{x}_R) - f_v(\boldsymbol{x}_L)}{\max\limits_{\boldsymbol{x}_j \in F_e} f_v(\boldsymbol{x}_j) - \min\limits_{\boldsymbol{x}_j \in F_e} f_v(\boldsymbol{x}_j)} & \text{(if both } \boldsymbol{x}_R \text{ and } \boldsymbol{x}_L \text{ exist)} \\ \infty & \text{(otherwise)} \end{cases} . \tag{13}$$

2. The nearest state vectors, $\bar{x}_{\mathrm{L}}, \bar{x}_{\mathrm{R}} \in F_e$, which give the positive minimum values of $f_{\mathrm{on}}(\bar{x}_{\mathrm{L}}) - f_{\mathrm{on}}(x_i)$ and $f_{\mathrm{on}}(x_i) - f_{\mathrm{on}}(\bar{x}_{\mathrm{R}})$, respectively, are first searched and, subsequently, $d_{\mathrm{on}}(x_i)$ is calculated by

$$d_{\mathrm{on}}(x_i) = \begin{cases} \dfrac{f_{\mathrm{on}}(\bar{x}_{\mathrm{R}}) - f_{\mathrm{on}}(\bar{x}_{\mathrm{L}})}{\min\limits_{x_j \in F_e} f_{\mathrm{on}}(x_j) - \max\limits_{x_j \in F_e} f_{\mathrm{on}}(x_j)} & \text{(if both } \bar{x}_{\mathrm{R}} \text{ and } \bar{x}_{\mathrm{L}} \text{ exist)} \\ \infty & \text{(otherwise)} \end{cases} . \quad (14)$$

3. The crowding distance $d(x_i)$ is evaluated as $d(x_i) = d_{\mathrm{v}}(x_i) + d_{\mathrm{on}}(x_i)$.

Like the case of the weighted GA in 3.2, the offspring state vectors are produced by using the uniform crossover and, subsequently, they are mutated randomly. In the NSGA-II, the number of state vectors in the parent population is assumed to be equal to that in the offspring one, and it is denoted by N_{pop}.

4. Numerical Results

Throughout the present study, the geometrical and physical parameters are fixed as follows: $R = 4$ cm, $b = 1$ mm, $z_0 = 1$ mm, $j_{\mathrm{C}} = 1$ MA/cm^2, $E_{\mathrm{C}} = 1$ mV/m, $N = 20$, $m = 10$ g, $R_1 = 5$ cm, $R_2 = 7$ cm, $H_{\mathrm{M}} = 10$ cm, $\alpha = 20$ kA/ms, and $z_{\mathrm{limit}} = 30$ cm. Moreover, the number n of current loops is fixed as $n = 100$. In addition, the division numbers in the on-off method are fixed as follows: $N_r = 4$ and $N_z = 20$. Namely, the number K of filaments is fixed as $K = 80$. Furthermore, the parameters in the weighted GA and the NSGA-II are fixed as follows: $N_{\mathrm{p}} = 20$, $N_{\mathrm{o}} = 100$, $N_{\mathrm{pop}} = 100$, and $s_{\mathrm{max}} = 2000$. Moreover, 5% of the offspring state vectors are selected randomly, and 20% of the genes in each selected vector are mutated randomly.

4.1. Optimization of Current Distribution in Electromagnet

4.1.1. Optimization by Weighted GA

Let us perform the current distribution optimization in the electromagnet by using the GA-based on-off method. First, we apply the weighted GA to the current distribution optimization. The combined objective function f, the speedup ratio f_{v}, and the on-ratio f_{on} are determined as a function of the generation s, and they are depicted in Fig. 3. Although f increases monotonously with s (see Fig. 3(a)), neither a completely monotonous increase in f_{v} nor a completely monotonous decrease in f_{on} can be obtained (see Fig. 3(b)). For example, a sudden decrease in f_{v} and a sudden increase in f_{on} are observed at $s = 1000$ and $s = 900$, respectively. This is because f_{v} is coupled to f_{on} through the weighting coefficient ω. Figures 3(a) and 3(b) also indicate that, finally, f_{v} and f_{on} reach up to 1.33 and down to 0.83, respectively.

Next, we investigate the influence of ω on the acceleration performance of the SLA system. To this end, the convergence values of f_{v} and f_{on} are determined as a function of ω, and they are plotted in Fig. 4. Both f_{v} and f_{on} almost vanish for the case with $\omega \lesssim 0.5$

(a) Combined objective function f.

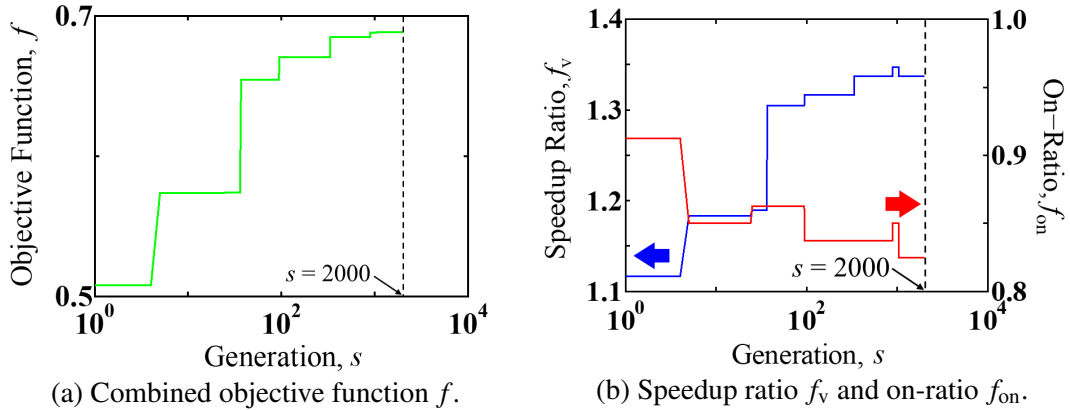(b) Speedup ratio f_v and on-ratio f_{on}.

Figure 3: Values of the objective functions during the optimization by the weighted GA for the case with $\omega = 0.7$. In Fig. 3(b), the blue and red lines show the speedup ratio f_v and the on-ratio f_{on}, respectively.

because the minimization of f_{on} is prioritized for this case. In contrast, f_v ~~takes almost the same value~~ for the case with $\omega > 0.5$. ~~Similarly, f_{on} takes almost the same value for $\omega > 0.5$.~~ This result implies that, ~~when the maximization of f_v is prioritized,~~ the values of (f_v, f_{on}) ~~for any other optimized solutions~~ might be ~~about~~ $(1.3, 0.8)$. This figure also shows that f_v takes the maximum for $\omega \simeq 0.7$. For this reason, ω is fixed as $\omega = 0.7$, hereafter.

4.1.2. Optimization by NSGA-II

We also apply the NSGA-II to the current distribution optimization. Throughout the present study, the optimized state vector $\boldsymbol{x}_{opt}$ means the state vector which takes the maximum of f_v among all state vectors in F_1. The speedup ratio $f_v(\boldsymbol{x}_{opt})$ and the on-ratio $f_{on}(\boldsymbol{x}_{opt})$ are determined as a function of the generation s, and they are depicted in Fig. 5. The speedup ratio f_v increases monotonously with s until it converges to 1.31. In contrast, the on-ratio f_{on} decreases monotonously with increasing generation number s until it converges to 0.85. Figures 3(b) and 5 show that, after the final ~~variations~~ of f_v and f_{on} at $s = 1000$, ~~the values of f_v and f_{on} take~~ the constant ~~until $s = 2000$,~~ Accordingly, it can be considered that ~~the values of~~ f_v and f_{on} converge at $s = 2000$. We also see from these figures that almost the same convergence values of (f_{on}, f_v) are obtained both for the weighted GA and for the NSGA-II. Therefore, both the solution of the weighted GA and that of the NSGA-II are quasi-optimized solutions ~~rather than locally optimized solutions~~.

Next, the current distribution obtained by the NSGA-II is compared with that by the weighted GA. The optimized current distributions by two types of GAs are shown in Fig. 6. Although the convergence values of (f_{on}, f_v) obtained by the NSGA-II are nearly equal to those by the weighted GA, the optimized current distributions by two types of GAs are widely different from each other. This result indicates that there exist multiple quasi-optimized solutions which show almost the same acceleration performance.

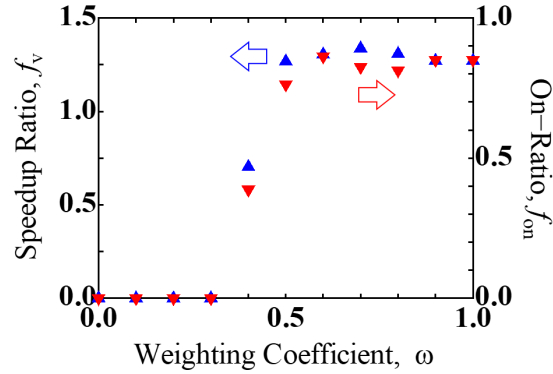Finally, the relationship between f_v and f_{on} is investigated. The values of (f_{on}, f_v) for

Figure 4: Convergence values of the speedup ratio f_v and the on-ratio f_{on} as a function of the weighting coefficient ω. Here, the blue and red triangles indicate values of f_v and those of f_{on}, respectively.
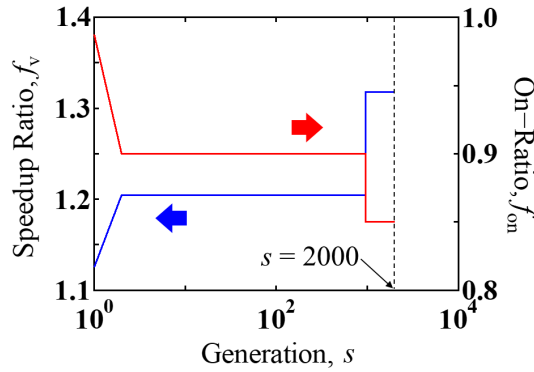

Figure 5: Values of the speedup ratio f_v and the on-ratio f_{on} during the optimization by the NSGA-II. Here, the blue and red lines show values of f_v and those of f_{on}, respectively.

all the state vectors in F_1 at $s = s_{max}$ are plotted in Fig. 7. The values of (f_{on}, f_v) for the optimized solution obtained by the weighted GA are also plotted in this figure. We see from this figure that, for the case with $f_{on} > 0.55$, the final velocity for the optimized current distribution is faster than that for the homogeneous current distribution. From the above result, we can conclude that, in designing the SLA system, an electric current should not be always applied to an entire electromagnet.

4.2. Analysis of Acceleration Performance

Let us first investigate the acceleration performance for the optimized current distributions obtained in 4.1. To this end, the velocity v is determined as functions of the film position Z and is depicted in Fig. 8. This figure shows $v_f = 110$ m/s and $v_f = 145$ for the homogeneous and optimized current distributions, respectively. Thus, the acceleration performance is considerably improved by using the optimized current distribution.
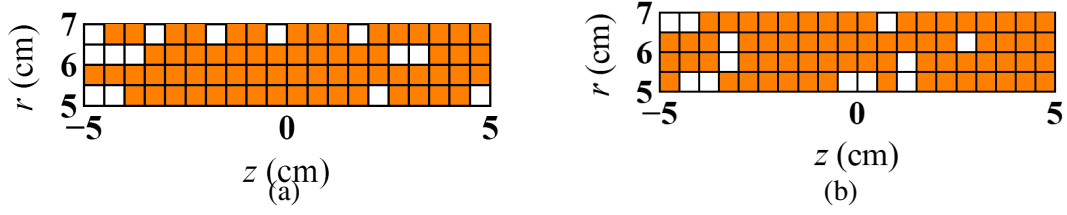
Figure 6: Optimized current distributions obtained by (a) the weighted GA and by (b) the NSGA-II. In these figures, the orange and white squares show on-state and off-state filaments, respectively.
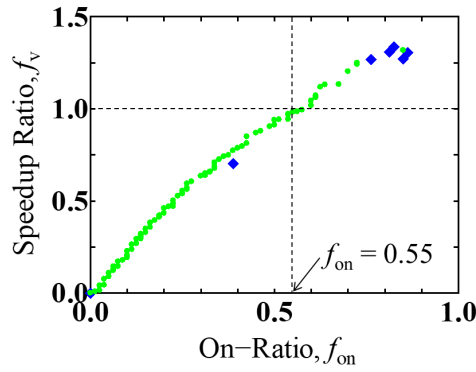

Figure 7: Dependence of the speedup ratio f_v on the on-ratio f_{on}. Here, the blue diamonds and the green circles show the values of (f_{on}, f_v) obtained by the weighted GA (with $\omega = 0.7$) and those by the NSGA-II, respectively.

Next, we investigate why the acceleration performance is enhanced by the optimized current distribution. To this end, Z-dependences of the total shielding current $I(t) \equiv \sum_{i=1}^{n} I_i(t)$ and r-component $B_r(Z, R, t)$ of the magnetic flux density are numerically determined both for the optimized current distribution and for the homogeneous one, and they are depicted in Figs. 9(a) and 9(b). We see from these figures that both $|I|$ and B_r become larger by using the optimized current distribution. As is apparent from the energy conservation law[1] corresponding to (7), an increase in both $|I_i|$ and B_r will rise the final velocity v_f. Therefore, the enhancement of the acceleration performance by the optimized current distribution might be attributable to an increase in both $|I_i|$ and B_r.

---

[1]From a straightforward calculation, the following energy conservation law can be obtained from (7):

$$\frac{1}{2}mv_f^2 = -2\pi \sum_{i=1}^{n} r_i \int_{z_0}^{z_{\text{limit}}} B_r(Z, r_i, t)I_i(t)\, dZ.$$

Note that $Z(t)$ is a monotonously increasing function of t. In other words, t is also a monotonous increasing function of the film position Z. Hence, $B_r(Z, r_i, t)$ is a function of Z and r_i, whereas $I_i(t)$ is a function of Z.
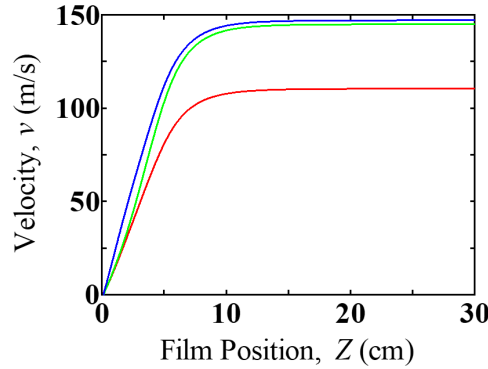
10

Figure 8: Dependence of the velocity *v* on the film position *Z*. In Figs. 8 and 9, the blue and green curves denote the values for the current distribution optimized by the weighted GA and those by the NSGA-II, respectively. In addition, the red curves denote the values for the homogeneous current distribution.

5.   Conclusion

By using the GA-based on-off method, we have optimized the current distribution in the electromagnet so as to maximize the acceleration performance of the SLA system. As an optimization method, the weighted GA and the NSGA-II are adopted. Conclusions obtained in the present study are summarized as follows:

1. There exist multiple quasi-optimized solutions which show almost the same acceleration performance, but their current distributions are totally different from one another.

2. An electric current should not be always applied to an entire electromagnet to achieve the quasi-optimized acceleration performance.

3. By optimizing the current distribution optimization in the electromagnet, the final velocity is improved by a factor of 1.3 as compared with that for the homogeneous current distribution.

The above conclusions could not be obtained without any optimization method. In this sense, the optimization strategy might be a powerful tool for the engineering design of the SLA system.
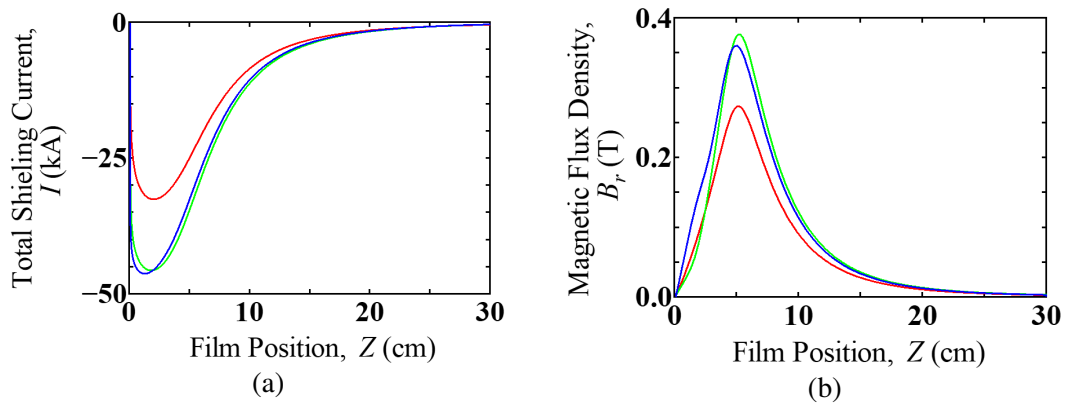
Acknowledgement

Figure 9: Dependences of (a) the total shielding current I and (b) r-component $B_r(Z, R, t)$ of the magnetic flux density on the film position Z.

References

[1] P. B. Parks, R. J. Turnbull: Effect of transonic flow in the ablation cloud on the lifetime of a solid hydrogen pellet in a plasma, *Phys. of Fluids*, 20 (1978), 1735–1741.

[2] S. L. Milora, C. A. Foster: A revised neutral gas shielding model for pellet-plasma interactions, *IEEE Trans. Plasma Sci.*, 6:4 (1978), 578–592.

[3] R. Sakamoto, H. Yamada: Fueling requirements of super-high-density plasmas towards innovative ignition regime, *Fusion Eng. Des.*, 89:6 (2014), 812–817.

[4] N. Yanagi, G. Motojima: private communication, National Institution for Fusion Science (2017).

[5] T. Yamaguchi, T. Takayama, A. Saitoh, A. Kamitani: Comparison between FEM and equivalent-circuit model simulations of superconducting linear acceleration system for pellet injection, *J. Adv. Simulat. Sci. Eng.*, 4:2 (2017), 209–222.

[6] T. Yamaguchi, T. Takayama, A. Saitoh, A. Kamitani: Numerical investigation on superconducting linear acceleration system for pellet injection by using equivalent-circuit model, *IEEE Trans. Magn.*, 55:6 (2019), Art no. 7204305.

[7] L. Makong, A. Kameni, P. Masson, J. Lambrechts, F. Bouillault: 3-D modeling of heterogeneous and anisotropic superconducting media, *IEEE. Trans. Magn.*, 52:3 (2016), Art. no. 7205404.

[8] A. Kamitani, T. Takayama, A. Saitoh, H. Nakamura: High-speed algorithm for shielding current analysis in HTS film with cracks, *Plasma Fusion Res.*, 10 (2015), Art. no. 3405023.

[9] W. H. Press, S. A. Teukolsky, W. T. Vetterling, B. P. Flannery: Numerical Recipes in Fortran 77, *Cambridge Univ. Press*, New York, USA, 1992.

[10] A. Kamitani, T. Takayama, H. Nakamura: High-performance analysis of shielding current density in high-temperature superconducting thin film, *Plasma Fusion Res.*, 5 (2010), Art. no. S2112.

[11] K. Deb, A. Pratap, S. Agarwal, T. Meyarivan: A fast and elitist multiobjective genetic algorithm: NSGA-II, *IEEE Trans. Evol. Comput.*, 6:2 (2002), 182–197.